Alfvén Eigenmode dynamics during the recent operational phase at the Wendelstein 7-X stellarator

K. Rahbarnia[1], S. Vaz Mendes[1], C. Büschel[1], C. Brandt[1], H. Thomsen[1], A. von Stechow[1], J.-P. Bähner[2], S.K. Hansen[2], R. Kleiber[1], C. Slaby[1], A. Könies[1] and Wendelstein 7-X Team

[1]*Max-Planck-Institut für Plasmaphysik, Greifswald, Germany*

[2]*Massachusetts Institute of Technology, Cambridge, Massachusetts, USA*

Fluctuation measurements in ECRH and NBI plasmas

During the recent operational phase OP 2.1, magnetic and density fluctuations were studied in a large number of experiments. Figure 1 provides an overview of observations made by different fluctuation diagnostics. The depicted frequency spectra are measured in a specific plasma heating set-up (PID 20230214.035), which combines O2-ECRH and NBI to reach a high energy and good confinement regime, the so-called high-performance plateau. Figure 1a depicts a frequency spectrum of a selected Mirnov coil [1,2], where a broadband structure ~200 kHz is marked. This is a well-known Wendelstein 7-X (W7-X) plasma feature, which was studied extensively in the past [1,3]. It originates from elliptically or helically induced Alfvén Eigenmodes (AE), which are strongly interlinked with observed ITG turbulence [3,4]. Additionally in figure 1a a chirping mode activity ~ 350 kHz and narrowband low frequency fluctuations ~ 10 kHz are labelled. Both features are also observed by measurements with the soft X-ray camera system [5] (figure 1b) and the phase contrast imaging diagnostic [4] (figure 1c). The

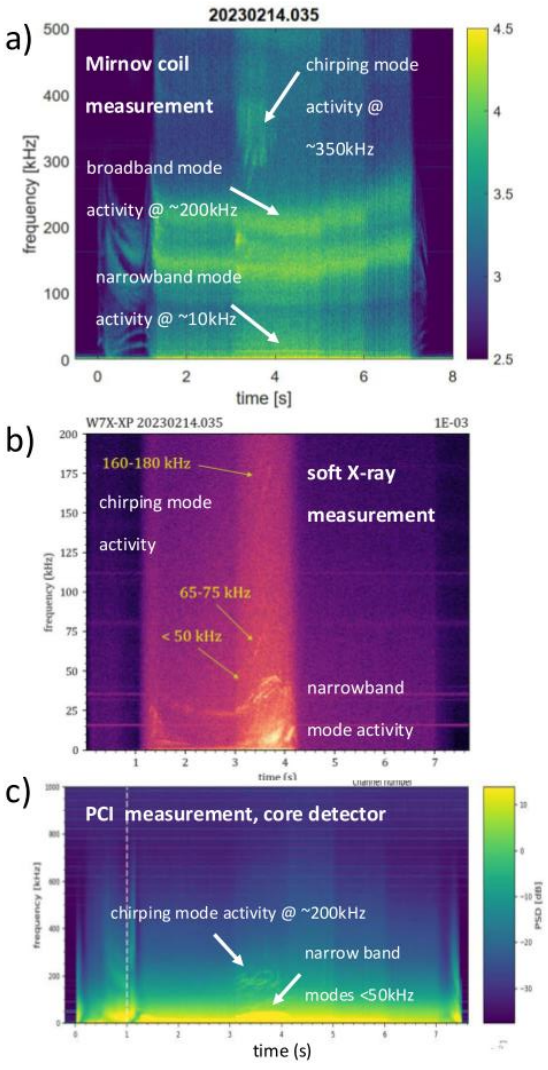

Figure 1: *Example of fluctuation measurements of various diagnostics (PID 20230214.035, high performance plateau from 3-4s): Mirnov coil (a), soft-X-ray (b) and phase contrast imaging (c). Similar features within the FFT-frequency spectra are labelled.*

corresponding phenomena are marked in the spectra, respectively. It is noted that the frequencies do not match perfectly across diagnostics. Whether they actually have the same origin is currently under investigation.

Magnetic fluctuations in low power ICRH plasmas

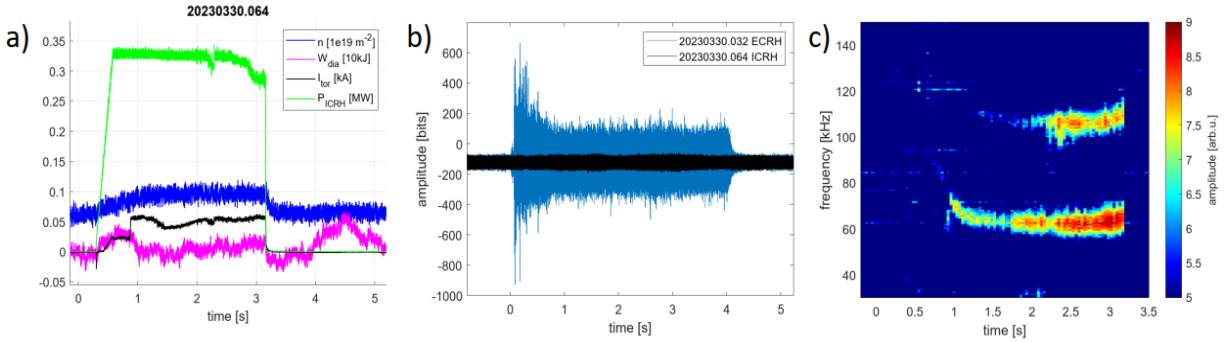

Figure 2: *Example of a magnetic fluctuation measurement during a pure low power ICRH plasma pulse (PID 20230330.064): a) time traces of line-integrated density, diamagnetic energy, toroidal plasma current and ICRH power, b) comparison of a Mirnov coil signal measured in an ECRH (blue) and low power ICRH plasma (black), c) frequency spectrum of the pure ICRH Mirnov coil signal shown in b) (calculated with DMusic)*

For the first time at W7-X a pure ICR heated plasma has been ignited and diagnosed (PID 20230330.064). The ICRH power was fairly low (~300 kW) and most standard diagnostics were not able to detect a meaningful signal (figure 2a). A comparison of the fluctuating raw data of a selected Mirnov coil, clearly shows a very weak pick-up in case of the low power ICRH plasma (figure 2b, blue: Mirnov signal in ECRH plasma, black: same coil, but ICRH plasma). The corresponding frequency spectrum (calculated with DMusic [6]) shows two narrowband structures at ~110 kHz and ~61 kHz (figure 2c). A follow-up mode analysis by using the SSI-method [6] reveals modes with a poloidal mode number of m = -2 and m = -1 for f = 110 kHz and f = 61 kHz (figure 3), respectively. In future campaigns the

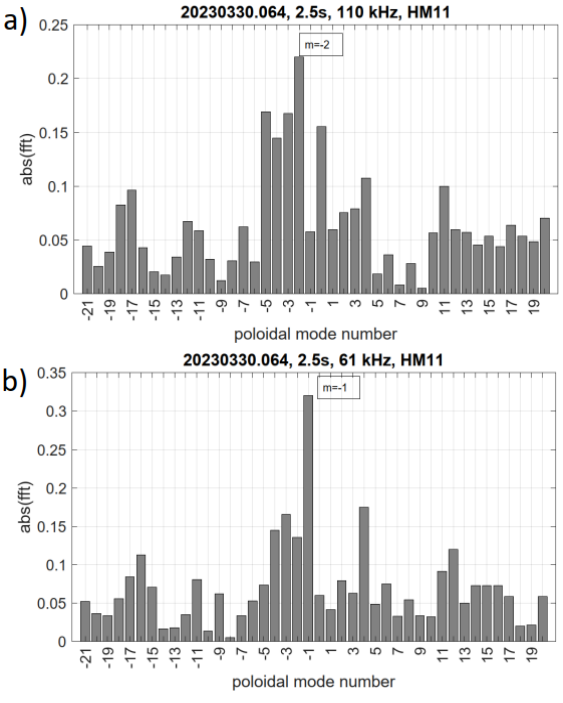

Figure 3: *Experimental mode spectra calculated for f = 110 kHz (a) and f = 61 kHz (b) of the magnetic fluctuations measured by 41 poloidally arranged Mirnov coils in half module 11 (PID 20230330.064).*

ICRH power will be significantly higher and resulting fast ion driven modes will be investigated further.

Synthetic Mirnov diagnostic

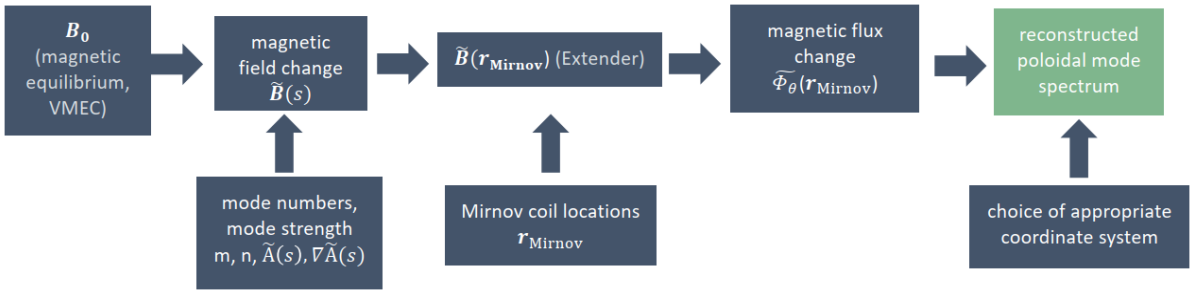

Figure 4: *Schematic overview of the synthetic diagnostic*

A synthetic Mirnov diagnostic has been developed in order to explore a number of aspects, which are important to analyse and understand the experimental mode spectra, i.e. the effect of the magnetic field configuration, the Mirnov coil arrangement geometry, the resolvable mode number range, mode coupling effects and the choice of an appropriate coordinate system. A schematic overview in figure 4 illustrates the necessary quantities and internal workflow to reconstruct a poloidal mode spectrum for a given Mirnov coil arrangement [7]. The initial starting point is a given poloidal mode strength and number, either from artificial data, or a pre-calculated data set, which is derived from calculations with the 3D-MHD continuum codes CAS3D [8] and CKA [9]. The magnetic flux change is calculated at the locations of the actual Mirnov coils based on VMEC [10] and the Extender module. Finally the same mode analysis technique as in case of experimental data is performed to get the poloidal mode spectrum. As depicted in figure 5, a measured mode spectrum (figure 5a) is reconstructed by the synthetic diagnostic (figure 5b) for a given mode with poloidal mode numbers m = 2,4. Furthermore an extensive parameter study specifically made for the W7-X case confirms the

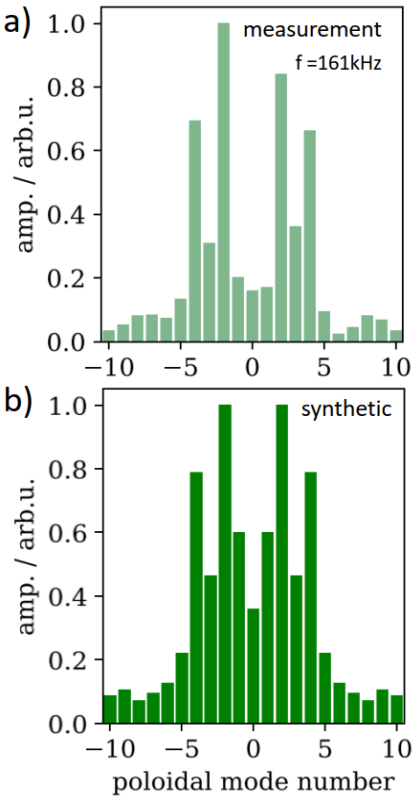

Figure 5: *The measured mode numbers can be reconstructed by the synthetic Mirnov diagnostic (b) for the observed m = 2, 4 modes (a).*

optimal design of the Mirnov coil arrangement in half module 11 for the so-called magnetic standard configuration [11,12] (figure 6). Also it is found that the most suitable choice for mode spectra evaluation and comparison are geometrical torus coordinates. The actual mode number resolution is limited by a multipole decay proportional to $1/r^{m+1}$ (r - minor radius, m – poloidal mode number) and depends on the magnetic configuration (standard: m < 7, high iota: m < 5).

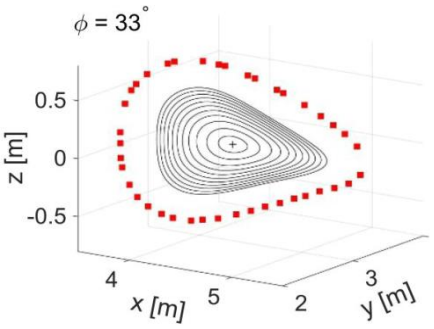

Figure 6: *41 Mirnov coils in half module 11 (red squares). In black, flux surfaces of the standard configuration are shown.*

This work has been carried out within the framework of the EUROfusion Consortium, funded by the European Union via the Euratom Research and Training Programme (Grant Agreement No 101052200 — EUROfusion). Views and opinions expressed are however those of the author(s) only and do not necessarily reflect those of the European Union or the European Commission. Neither the European Union nor the European Commission can be held responsible for them.

Support for the MIT participation was provided by the US Department of Energy, Grant DE-SC0014229.

References

[1] K. Rahbarnia et al., Nucl. Fusion, Vol. 58, 096010 (2018)

[2] M. Endler et al., Fusion Eng. and Design, Vol. 100, pp 468 (2015)

[3] S. vaz Mendes et al., submitted to Nuclear Fusion (2023)

[4] A. von Stechow et al., arXiv preprint arXiv:2010.02160 (2020)

[5] C. Brandt et al., Fusion Eng. and Design, Vol. 123, pp 887 (2017)

[6] R. Kleiber et al., Plasma Phys. Control. Fusion 63 035017 (2021)

[7] C. Büschel, Master Thesis IPP Greifswald (2023)

[8] C. Nührenberg, Physics of Plasmas, 6(1):137–147, 01 (1999)

[9] A. Könies, 10th IAEA TM on Energetic Particles in Magnetic Confinement Systems Germany: Kloster Seeon (2007)

[10] S.P. Hirshman and J.C. Whitson, Phys. Fluids 12 3553 (1983)

[11] T. Andreeva et al., Plasma Phys. 4 45–7 (2002)

[12] J. Geiger et al., Plasma Phys. Control. Fusion 57 014004 (2015)